Dalton Transactions

ROYAL SOCIETY OF CHEMISTRY

PAPER

View Article Online
View Journal | View Issue

Check for updates

Cite this: *Dalton Trans.*, 2025, **54**, 8445

Highly tenebrescent hackmanites from natural nepheline†

Cecilia Agamah, [a,b] Sami Vuori, [a] Ermei Mäkilä, [c] Anssi Peuronen [a] and Mika Lastusaari *[a]

Received 18th February 2025,
Accepted 21st April 2025

DOI: 10.1039/d5dt00389j

rsc.li/dalton

Photochromic hackmanites, $(Na,K)_8Al_6Si_6O_{24}(Cl,S)_2$, were synthesized with a solid state reaction route using natural nepheline, $(Na,K)AlSiO_4$, as a starting material together with NaCl, KCl and Na_2SO_4. The hackmanite was obtained using NaCl, whereas with KCl the nepheline reacted only partially. In particular, materials synthesized with NaCl showed a deep photochromic color under UV irradiation and good sensitivity to even low solar UV index values. This suggests that the material is well suited for personal solar UV exposure monitoring.

1 Introduction

Photochromic materials, otherwise known as tenebrescent materials, exhibit reversible color changes when exposed to radiation of different wavelengths. They can be employed in filters,[1] optical information storage,[2] biomedicine,[3] and textile industry[4] to mention a few. Both organic and inorganic photochromic compounds or even their hybrids have been studied.[5–8] While most photochromic organic compounds have limitations in durability, inorganic photochromes maintain functionality even under harsher conditions. However, unlike their organic counterparts, the classic inorganic photochromic materials like WO_3,[9,10] MoO_3,[11] V_2O_5,[12] ZnO and TiO_2[13] are typically difficult to tune in terms of color or energy required to induce the color change. Furthermore, some recent inorganic photochromic materials such as $ErNbO_4$ and $YbNbO_4$[14] are rare-earth doped, raising the cost of production. Of interest, though, are photochromic synthetic hackmanites, based on the mineral hackmanite $Na_8Al_6Si_6O_{24}(Cl,S)_2$, which is the photochromic form of the mineral sodalite,[15] $Na_8(Al_6Si_6O_{24})Cl_2$. This compound is durable and offers the possibility of excluding lanthanides and heavy metals,[16] with varied synthesis routes[17–21] tailored towards desired results. Moreover, they have tunable photochromic properties.[22]

The mechanism of tenebrescence in hackmanites is based on color centers (also called F-centers) formed when electrons transfer from (di)sulfide ions (S_2^{2-}) and are trapped in Cl vacancies (V_{Cl}) when the hackmanite sample is irradiated with UV or higher energy radiation. To reverse the process, the sample is exposed to visible light or heating.[21–24]

Hackmanites have been successfully synthesized in the lab by using mainly alkali halides, zeolite A and a sulphate containing compound (*e.g.* Na_2SO_4). Of significant importance is the variation of starting materials in its synthesis. This allows for the photochromism to be tuned by changing or substituting constituent atoms or doping for desired applications.[21] So far, varying starting materials mainly concern alkali halides and sometimes Al and Si,[21,23,25] and omitting the zeolite A.[19] Chang[26] described a method of synthesizing photochromic and cathodochromic sodalites (general name for hackmanites) which he called the structure conversion method (SCM). As the name implies, a complex sodium–aluminosilicate complex (Na–Al–silicate) which has a basic building block of a tetrahedron with a small silicon or aluminium ion enclosed in four oxygen ions, is converted to the sodalite structure. The tetrahedra are similar to those in the sodalite but "distorted" giving room for the incorporation of alkali halides and sulfur containing compounds to synthesize sodalites. The sodium–aluminosilicate complex they used was zeolite A ($NaAlSiO_4$).

Synthetic hackmanites have gained popularity in recent years due to their ease of synthesis, cost effectiveness, environmental friendliness and the various possible applications based on tenebrescence. These include detection of X-ray doses and photochromic X-ray imaging,[27] UV dosimetry and solar UV index measurement,[28] blue light dosimetry[29] and photochromic photography.[30] Despite all these attractive features, synthetic hackmanites still lack the ability of natural hackmanites to change color efficiently in sunlight, even if some coloration can be obtained.

It is known that the coloration threshold wavelength can be tuned by adjusting the size of the color center, and especially

[a]*University of Turku, Department of Chemistry, FI-20014 Turku, Finland. E-mail: miklas@utu.fi*
[b]*University of Turku Graduate School (UTUGS), Doctoral Programme in Exact Sciences (EXACTUS), FI-20014 Turku, Finland*
[c]*University of Turku, Department of Physics and Astronomy, FI-20014 Turku, Finland*
† Electronic supplementary information (ESI) available. See DOI: https://doi.org/10.1039/d5dt00389j

replacing Na with K will shift the threshold to match with the human erythemal action spectrum.[28] Since only quite low potassium concentrations have been obtained with regular laboratory synthesis methods, in this work we use natural nepheline from Canada as the starting material to synthesize hackmanites. Nepheline has the nominal composition $Na_3KAl_4Si_4O_{16}$, thus providing a good alternative for zeolite A ($NaAlSiO_4$) commonly used in the solid state synthesis of hackmanites. Moreover, natural nepheline is currently used, for example, in the glass and ceramics industries,[31,32] so there is already infrastructure for its mining and processing. Also, using a natural mineral instead of a highly processed chemical will potentially reduce the energy footprint of production.

2 Experimental

2.1 Sample preparation

The Na and K hackmanite samples were synthesized by solid-state reactions using stoichiometric amounts of natural nepheline $Na_{2.01}K_{0.96}Ca_{0.04}Al_{3.55}Si_{4.57}O_{16}$ (this composition was determined experimentally; see section 3.1), NaCl (VWR chemicals, 99.8%) or KCl (E. Merck, 99.5%), and Na_2SO_4 (E. Merck, 99%) as starting materials. A 7.5 times stoichiometric excess of NaCl and 3.25 times excess of KCl were used for the syntheses to help the formation of the hackmanite phase. Na_2SO_4 was used in a 1 : 10 stoichiometric ratio with respect to NaCl or KCl.

The materials were ground and heated at 850 °C in air for 48 h after which they were allowed to cool down to room temperature and ground. The mixture was then reheated for 2 h under a N_2/H_2 (88%/12%) atmosphere and allowed to freely cool down and then ground in an agate mortar. The product was then washed with water to remove any excess NaCl and/or KCl impurities.

2.2 Characterization

The structure and purity of the samples were determined by X-ray powder diffraction measurements using either a Huber G670 detector and Cu $K_{\alpha1}$ radiation (λ = 1.54060 Å) or a PANalytical Aeris diffractometer and Cu $K_{\alpha1,2}$ radiation (λ = 1.54060 and 1.54439 Å). From these data, unit cells were refined with FullProf[33] or PANalytical HighScore, respectively. The samples' compositions and X-ray-induced coloring were investigated using X-ray fluorescence spectroscopy (XRF) with a PANalytical Epsilon 1 instrument with its internal Omnian calibration. The device uses an Ag X-ray tube with characteristic K emission at *ca.* 22 keV.

The composition of the samples was further studied using energy-dispersive X-ray spectroscopy (EDS) coupled with scanning electron microscopy (SEM). For analysis, the samples were prepared by embedding an amount of powder in Petropoxy 154 epoxide resin (Burnham Petrographics). The resin block was then cross-sectioned using an argon Broad Ion Beam mill with a 5 kV acceleration voltage (ArBlade 5000, Hitachi High-Technologies). The obtained cross section was analyzed in an Apreo S field-emission SEM (Thermo Scientific) equipped with an UltimMax 100 EDS detector (Oxford Instruments). The EDS measurements were carried out using an acceleration voltage of 20 kV under a low vacuum of 90 Pa H_2O, with the elemental composition estimated using the built-in standardless approach.

Single-crystal X-ray diffraction data were collected with a Bruker–Nonius Kappa ApexII diffractometer using Mo $K_{\alpha1}$ radiation (λ = 0.71073 Å). COLLECT, HKL Denzo and Scalepack software were used for data collection and reduction,[34,35] respectively. The structure was solved and refined within Olex2 GUI[36] using SHELXS and SHELXL programs.[37,38]

Crystal data for $Al_4Ca_{0.09}K_{0.56}Na_{3.28}O_{16}Si_4$ (M = 576.68 g mol^{-1}): hexagonal, space group $P6_3$ (no. 173), $a = b$ = 9.9847(2) Å, c = 8.3726(2) Å, V = 722.87(3) Å^3, Z = 2, T = 170.0(10) K, μ(MoKα) = 1.037 mm^{-1}, D_{calc} = 2.649 g cm^{-3}, 7559 reflections measured ($4.71° \leq 2\theta \leq 60.054°$), 1407 unique ($R_{int}$ = 0.0263, R_{sigma} = 0.0220) which were used in all calculations. The final R_1 was 0.0251 ($I > 2\sigma(I)$) and wR_2 was 0.0667 (all data).

The colors of the samples were investigated using a Konica Minolta handheld spectrometer (CM-2300d). They were first irradiated with a 4 W handheld, 254/365 nm UV lamp (UVLS-24) or a 6 W handheld, 302 nm UV lamp (UVM-57) for 5 min and 1 min, respectively, before the reflectance was measured. The color was again investigated with a LOT Quantum Design Solar simulator (LS0500/1) and the UV index values were measured with a Digital UV Radiometer model 6.5 UV Index. The samples were exposed to a UVI range of 1–15 and irradiated for 1 min before the reflectance measurement.

Tenebrescence excitation properties were investigated using a LOT MSH 300 monochromator with a 150 W Xe-Arc Lamp, coupled to an Avantes AvaSpec-HS-TEC spectrometer with an Avantes FC-IR600-1-ME-HTX optical fiber and Avantes AvaSoft 8.11.0.0 as the measurement software in reflectance mode. The white light source used was an Ocean Optics LS-1 Cal calibration lamp directed towards the sample, being 10 cm away. For each wavelength chosen, the samples were excited for 5 min with the LOT MSH 300 monochromator with wavelengths from 220 to 400 nm, followed immediately by data collection. The RGB values were obtained from the reflectance spectra using Osram color calculator software.[39]

The photoluminescence and persistent luminescence properties were studied at room temperature using a Varian Cary Eclipse fluorescence spectrophotometer equipped with a Hamamatsu R928 photomultiplier and a 15 W xenon lamp. For photoluminescence, the phosphorescence mode was used, with a total decay time of 0.005 s, a delay time of 0.1 ms, the number of flashes of 1, a data interval of 0.2 nm, a photomultiplier tube (PMT) voltage of 800 V, and excitation and emission slits of 10 nm and 2.5 nm, respectively. For persistent luminescence, a delay of 0.1 ms was used together with a 5 ms gate time with an emission slit of 20 nm, a data interval of 1.0 nm, and a (PMT) voltage of 800 V. The materials were irradiated with the handheld UV lamp for 5 min and a delay of 30s was applied before the persistent luminescence properties were investigated.

Luminance fading curves (persistent luminescence lifetimes) were measured at room temperature using a Hagner ERP-105 luminance photometer with a Hagner SD-27 detector coupled to a Fluke 189 multimeter. The samples were excited with 254 nm and 302 nm radiation from the previously described UV lamp for 30 minutes. After this, the measurements began immediately and continued until the luminance decreased to below 0.3 mcd m^{-2}.

3 Results and discussion

3.1 Phase purity and composition

A piece of nepheline from Canada (Fig. 1a) was bought from a private collector, and it did not show any photochromism. It was confirmed to be nepheline using X-ray powder diffraction (Fig. 1b), and the composition was observed to be approximately $Na_{2.01}K_{0.96}Ca_{0.04}Al_{3.55}Si_{4.57}O_{16}$ based on EDS analysis (Fig. 1c, S1 and S2;† Tables 1, S1 and S2†). Single-crystal X-ray diffraction analysis of a single crystal, chipped off from the nepheline sample, was carried out by solving and refining the structure in the $P6_3$ space group (Tables 2 and S3†). Based on the earlier literature, Na/K/Ca cation disorder was expected to manifest at the 0,0,*z* position and a disorder model was built by using the initial occupancies obtained from the EDS results. The cation occupancies and the *z* coordinates were first refined freely and then constrained to the obtained values yielding a composition of $Na_{3.27}K_{0.55}Ca_{0.09}Al_4Si_4O_{16}$. This composition is somewhat different from that obtained with EDS; the XRD data are from one crystal, whereas the EDS results are an average of multiple crystals. The obtained unit cell parameters are comparable to the powder XRD fitted unit cell (Tables 2 and S4 and Fig. S3†). These results indicated that the sample was as expected and thus it was used as the starting material in subsequent syntheses.

After the syntheses and washing with water to remove any soluble chlorides, the batches with NaCl and KCl as starting materials were analyzed for purity and composition. The diffraction patterns (Fig. 1d) show that each sample contains the expected hackmanite phase. The Na sample contains a trace amount of nepheline, whereas the K sample contains 52% hackmanite and 48% nepheline. The EDS analysis carried out for the Na material (Table 1) indicates a drastic decrease in the relative potassium content caused by the structural conversion from nepheline to sodalite: taking *e.g.* the sodium content as reference, the potassium concentration decreases by *ca.* 80% from that in the original nepheline. This is thus in good agreement with the poor solubility of potassium in sodalite.[28]

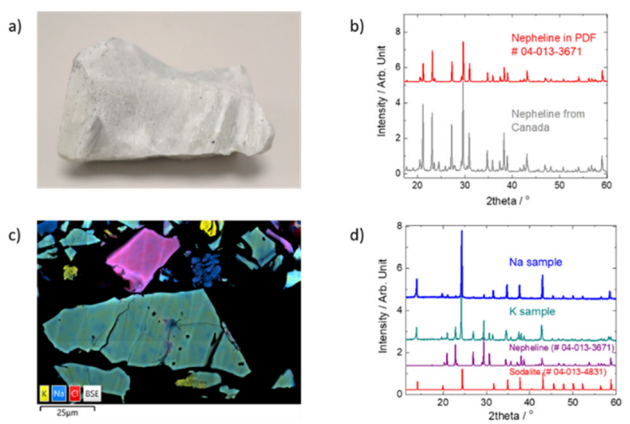

Fig. 1 (a) Photograph of the nepheline mineral used in this work. The mineral is *ca.* 8 cm in width. (b) X-ray powder diffraction analysis of the nepheline sample. (c) SEM-EDS elemental map for the nepheline sample. (d) X-ray powder diffraction analysis of the synthesized samples.

Table 1 Cation compositions (atom%) obtained with EDS analysis

Sample	Na	K	Ca	Al	Si	K to Na ratio
Nepheline	18.0	8.7	0.4	31.9	41.0	0.48
Na hackmanite	24.8	2.4	0.3	26.1	32.4	0.10

3.2 UV- and X-ray-induced tenebrescence

The synthesized samples were exposed to UV radiation from hand-held lamps of wavelengths 254, 302 and 365 nm as well as X-rays from a silver X-ray tube within an X-ray fluorescence spectrometer. A color change was observed in both compositions using all the mentioned irradiation (Fig. 2a and b).

Irradiation with the UV lamps yielded strong tenebrescence with 254 and 302 nm and weak tenebrescence with 365 nm and with X-rays. The Na sample reflectance curves are centered around 580 nm and with 254 and 302 nm they seem to contain two overlapping bands, at *ca.* 540 nm and 600 nm (Fig. 2a). This results in a bluish purple color (RGB 138, 54, 255). With 365 nm and X-rays, the band is a narrower single band at *ca.* 570 nm giving a purple color (RGB 211, 16, 255). For the K sample, the reflectance curves show a narrower minimum centered around 600 nm (Fig. 2b). Again, with 254 and 302 nm, the band is wider than with 365 nm and X-rays. The wider band shows a bluer purple color (RGB 106, 94, 255) and the narrower band shows a blue color (RGB 0, 156, 255). Overall, the Na material shows higher intensity in the color change than the K one as expected based on their phase purity. They both followed a similar pattern in terms of intensity: 302 nm > 254 nm > X-ray > 365 nm (Fig. 2c). It is to be noted that although there is a trace impurity of nepheline in the Na hackmanite, the UV sensitivity is not due to it, because the nepheline in itself is not tenebrescent.

3.3 Characteristics of color change

Because the K hackmanite material could not be synthesized in pure form, only Na materials were used to investigate the color change characteristics further. The tenebrescence excitation spectrum (Fig. 3a) indicates that the color change from white to blue/purple can be obtained with wavelengths below 400 nm. Similar to what was previously reported for natural hackmanites,[40] the excitation spectrum has two maxima, one in the UVC/UVB region and the other in UVA. It is especially notable that UVA (315–400 nm) colors the material well, which

Table 2 Refined unit cell parameters for nepheline and Na and K samples

	Nepheline – hexagonal ($P6_3$)			Hackmanite – cubic ($P\bar{4}3n$)		
	Single crystal	Powder	Ref.[a]	Na sample	K sample	Ref.[b]
a/Å	9.9847(2)	10.00226(7)	9.998	8.88877(4)	8.92066(1)	8.916
b/Å	9.9847(2)	10.00226(7)	9.998	8.88877(4)	8.92066(1)	8.916
c/Å	8.3726(2)	8.38577(5)	8.385	8.88877(4)	8.92066(1)	8.916
α/°	90	90	90	90	90	90
β/°	90	90	90	90	90	90
γ/°	120	120	120	90	90	90
Volume/Å^3	722.87(3)	726.56	725.87	702.30(1)	709.89(1)	708.78

[a] Composition: $Na_{2.93}K_{0.88}Ca_{0.065}Al_{3.94}Si_{4.06}O_{16}$ (PDF #04-013-3671). [b] Composition: $Na_8Al_6Si_6O_{24}Cl_2$ (PDF #04-013-4831).

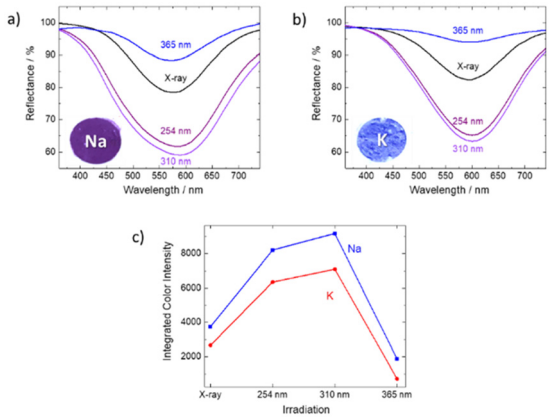

Fig. 2 Reflectance spectra (a) for the Na sample and (b) the K sample. The inset photographs indicate the photochromic color observed for the materials irradiated with 302 nm. (c) Comparison of the color intensities of the samples after different irradiation.

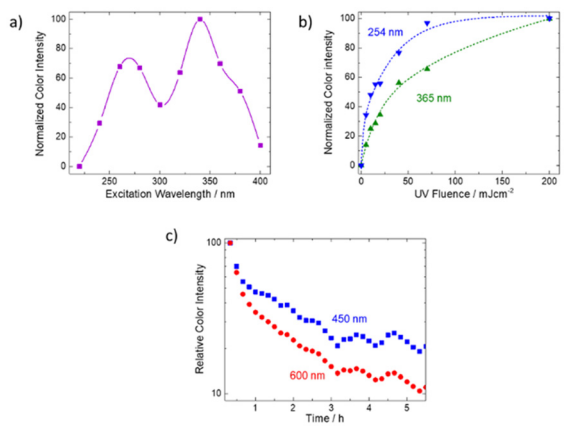

Fig. 3 (a) Tenebrescence excitation spectrum, (b) color rise under different irradiation wavelengths and (c) color fade curves under white LED light at two different wavelengths. All data are for the Na material.

is rare in hackmanite materials synthesized from commercial starting materials. Since the synthesis route employed in this work involves the collapse of the hexagonal nepheline structure[41] and the subsequent buildup of the cubic sodalite structure,[42] we can assume that also the original defect structure of the nepheline will collapse. This suggests that the ability to change color under UVA irradiation is controlled more by elemental and defect composition than by how much time the defect structure has to reach an equilibrium. The latter has previously been considered as one possible reason for natural samples being more sensitive to UVA than synthetic ones.

Because of the twin peak shape of the excitation spectrum, we recorded color rise curves for both UVC (254 nm) and UVA (365 nm) (Fig. 3b). The results indicate that with UVC irradiation the color intensity increases faster than with UVA. Then, we recorded the fading of the color under normal laboratory white LED lighting and observed that the color faded faster at 600 nm than at 450 nm (Fig. 3c). As discussed above, absorption at 600 nm is obtained with both UVA and UVC excitation (see Fig. 2a: excitation at 254 or 365 nm gives a band at *ca.* 600 nm), while at 450 nm absorption is obtained with UVC only (see Fig. 2a: excitation at 254 nm does, but 365 nm does not yield a band at *ca.* 450 nm). This means that the coloration obtained with UVA fades more slowly than that obtained with UVC. Based on previously published work,[28] we assign the absorption band obtainable with UVA to a K rich local structure, and the UVC sensitive band to a Na rich one.

Because for a regular hackmanite ($Na_8Al_6Si_6O_{24}(Cl,S)_2$) the color center absorption is at *ca.* 550 nm, we assume that also in the present materials the 540 nm absorption corresponds to a Na rich color center. Thus, the 600 nm band would be due to a K rich color center. Then, based on the photochromism mechanism reported earlier[40] the present material's coloration process is as follows (Fig. 4): the activation is obtained with UV energies 3.3–4.1 eV (300–380 nm) for the K rich center and 4.1–5.2 eV (240–300 nm) for the Na rich center. This corresponds to a $^1[S_2^{2-},V_{Cl}(a_1)] \rightarrow {}^1[S_2^{-},V_{Cl}^{-}(a_1)]$ transition within the disulfide and the chloride vacancy pair. The system then relaxes to a $^3[S_2^{-},V_{Cl}^{-}(a_1)]$ state forming the color center. The K rich color center absorbs at 2.1 eV (600 nm) and the Na rich one at 2.3 eV (540 nm) due to a $^3[S_2^{-},V_{Cl}^{-}(a_1)] \rightarrow {}^3[S_2^{-},V_{Cl}^{-}(t_2)]$ transition.

3.4 Application as a solar UV index indicator

Previously, it has been reported that synthetic hackmanites can be utilized well for solar UV index (UV) indication only if

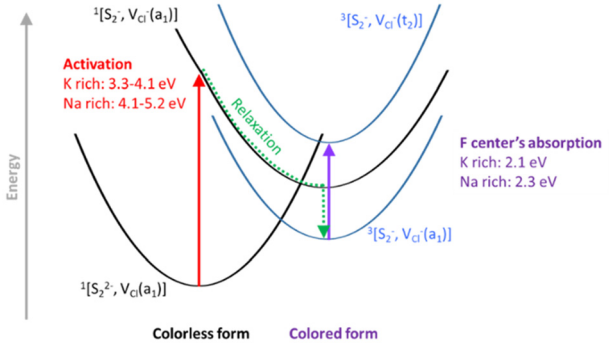

Fig. 4 Configurational coordination scheme of the photochromism in this work's hackmanites.

either a concentrating lens is used[27] or if the visible part of the spectrum is blocked.[43] Without these actions, the color would be very faint at any UVI.

In the present work, we observe that already at UV index 1, the material clearly changes color (Fig. 5a) when using a solar simulator lamp for one minute without any lenses or vis blocking filters. The color intensity reaches near saturation already at *ca.* UVI 4 (Fig. 5b). It is evident, though, that the color is far less intense than if regular hand-held UVC and UVB lamps are used for the coloration (see Fig. 2a). Considering that the World Health Organization recommends protection from sunlight at UV index values 3 and above,[44] the present material's color intensity is ideally sensitive for indicating when protection should be used.

Even if the color intensity saturates at UVI 4, the *L*a*b** coordinates show a change until *ca.* UVI 12 (Fig. 5c–e). The lightness still decreases and on the red–green axis, the color shifts towards green when the UVI increases. On the yellow–blue axis the evolution towards blue continues very smoothly until saturation at *ca.* UVI 12 (Fig. 5e). These indicate that the material stores information related to the UV index even beyond the saturation of the color intensity, *i.e.* the limit observable by the naked eye or a similar device (*e.g.* camera).

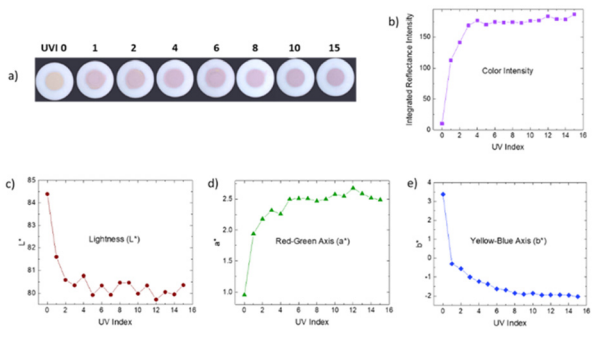

Fig. 5 (a) Photographs of the Na material after 1 min exposure to a solar simulator lamp at different UV index values. (b) Color intensity at different UVI values. (c)–(e) CIE *L*a*b** coordinates at different UVI values.

3.5 Luminescence properties

Because the K hackmanite material could not be synthesized in pure form, only Na materials (which had only trace impurities of nepheline) were used to investigate the luminescence characteristics. The Na materials' photoluminescence emission shows a wide band peaking in the blue range at 470 nm (Fig. 6a and b). This is at the same wavelength that has been reported earlier for synthetic hackmanites and assigned to the emission of a Ti^{3+} impurity.[23] Also, the excitation band peaking at 315 nm is at almost the same wavelength as reported for synthetic hackmanites.[23] Since the nepheline starting material is a natural mineral, there is the possibility of the presence of enough titanium to show luminescence, even though it might be below the detection limit of the EDS. It is also possible that this blue emission is due to oxygen defects as discussed by Finch *et al.*[45] As is often the case for synthetic hackmanites, the orange emission due to S_2^-, typical of natural hackmanites when excited with 365 nm,[46] seems to be missing from the present Na materials. Thus, the materials synthesized in this work behave more like synthetic than natural hackmanites when their photoluminescence is concerned.

Furthermore, persistent luminescence peaking at the same blue 470 nm wavelength was observed using excitation with hand-held UV lamps at 254, 302 and 365 nm (Fig. 6c). Like the photoluminescence emission, this band is due to Ti^{3+}. The delayed release of the excitation is due to trapping in oxygen vacancies and subsequent slow release from the traps.[46] The persistent emission lasts up to 12 min before reaching the photopic 0.32 mcd m^{-2} visibility limit set by DIN 67510-1[47] (Fig. 5d). This duration is very similar to that reported for natural hackmanites earlier.[46]

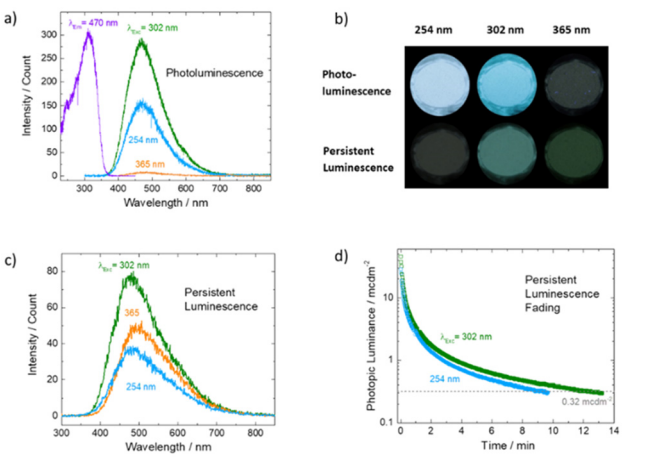

Fig. 6 (a) Photoluminescence excitation and emission spectra for the Na material. (b) Photographs of the photoluminescence and persistent luminescence obtained using different UV wavelengths and the same exposure parameters. (c) Persistent luminescence spectra and (d) fading curves for the Na material.

4 Conclusions

In this work, we report that photochromic hackmanites can be synthesized using natural nepheline as a starting material. Very deep coloration is obtained using hand-held UV lamps as excitation sources. We show that the hackmanite materials are very sensitive even to solar UV index values below 3, which makes the material a good candidate for personal solar UV exposure monitoring. The results thus suggest that the solar UV sensitivity typically found in natural hackmanites but lacking in synthetic ones is not due to a very long defect stabilization time, but rather the chemical composition.

Being able to use a natural starting material instead of highly processed synthetic chemicals promises a clear decrease in the energy footprint of producing photochromic hackmanites. Considering that nepheline is already mined commercially for use in glass and ceramic industries, its availability is already good. However, one must keep in mind that the composition of nepheline, especially the Na : K ratio, varies from one location to another.[48] Thus, the production of hackmanites with constant performance characteristics requires control of the source of nepheline.

Author contributions

Cecilia Agamah – investigation, data curation, formal analysis, writing – original draft, and writing – review & editing. Sami Vuori – investigation, data curation, formal analysis, and writing – review & editing. Ermei Mäkilä – data curation, formal analysis, investigation, and writing – review & editing. Anssi Peuronen – investigation, data curation, formal analysis, and writing – review & editing. Mika Lastusaari – conceptualization, formal analysis, funding acquisition, supervision, and writing – review & editing. The manuscript was written through the contributions of all authors. All authors have given approval to the final version of the manuscript.

Data availability

The data supporting this article have been included as part of the ESI.†

Conflicts of interest

There are no conflicts to declare.

Acknowledgements

We acknowledge the Materials Research Infrastructure (MARI) at the Department of Physics and Astronomy, University of Turku, for access and support with the broad ion beam and SEM facilities. We also acknowledge Mauri Nauma from the Department of Chemistry, University of Turku, for his help in grinding samples from the nepheline mineral.

References

1 T. W. Wysokinski, E. Czyzewska and A. H. Rawicz, *Thin Solid Films*, 1997, **295**, 31–36.
2 M. R. Tubbs and D. K. Wright, *Phys. Status Solidi A*, 1971, **7**, 155–166.
3 H. Cheng, J. Yoon and H. Tian, *Coord. Chem. Rev.*, 2018, **372**, 66–84.
4 S. M. R. Billah, R. M. Christie and R. Shamey, *Color. Technol.*, 2008, **124**, 223–228.
5 G. Xu, G. C. Guo, J. S. Guo, S. P. Guo, X. M. Jiang, C. Yang, M. S. Wang and Z. J. Zhang, *Dalton Trans.*, 2010, **39**, 8688–8692.
6 L. Liu, Q. Liu, Y. Q. Wei and G. C. Guo, *Inorg. Chim. Acta*, 2021, **519**, 120248.
7 Y. Badour, V. Jubera, I. Andron, C. Frayret and M. Gaudon, *Opt. Mater. Express*, 2021, **12**, 100110.
8 S. Helmy, F. A. Leibfarth, S. Oh, J. E. Poelma, C. J. Hawker and J. R. D. Alaniz, *J. Am. Chem. Soc.*, 2014, **136**, 8169–8172.
9 C. Azuma, T. Kawano, H. Kakemoto and H. Irie, *J. Appl. Phys.*, 2014, **116**(17), 173502.
10 S. Wang, W. Fan, Z. Liu, A. Yu and X. Jiang, *J. Mater. Chem. C*, 2018, **6**, 191.
11 T. He and J. Yao, *J. Photochem. Photobiol., C*, 2003, **4**, 125–143.
12 T. K. Le, P. V. Pham, C. L. Dong, N. Bahlawane, D. Vernardou, I. Mjejri, A. Rougier and S. W. Kim, *J. Mater. Chem. C*, 2022, **10**, 4019.
13 T. He and J. Yao, *Prog. Mater. Sci.*, 2006, **51**, 810–879.
14 Z. Zhang, L. Guo, H. Sun, D. Peng, H. Zou, N. Sun, Q. Zhang and X. Hao, *J. Mater. Chem. C*, 2021, **9**, 13841.
15 R. C. Peterson, *Can. Mineral.*, 1983, **21**, 549–552.
16 I. Norrbo, J. M. Carvalho, P. Laukkanen, J. Mäkelä, F. Mamedov, M. Peurla, H. Helminen, S. Pihlasalo, H. Härmä, J. Sinkkonen and M. Lastusaari, *Adv. Funct. Mater.*, 2017, **27**, 1606547.
17 J. M. Carvalho, I. Norrbo, R. A. Ando, H. F. Brito, M. C. A. Fantini and M. Lastusaari, *Chem. Commun.*, 2018, **54**, 7326.
18 D. B. Medved, *Am. Mineral.*, 1954, **39**, 615–629.
19 H. Byron, I. Norrbo and M. Lastusaari, *J. Alloys Compd.*, 2021, **872**, 159671.
20 E. F. Williams, W. G. Hodgson and J. S. Brinen, *J. Am. Ceram. Soc.*, 1969, **52**, 139–144.
21 E. R. Williams, A. Simmonds, J. A. Armstrong and M. T. Weller, *J. Mater. Chem.*, 2010, **20**, 10883–10887.
22 P. S. Pizany, M. C. Terrile, H. A. Farach and C. P. Poole, *Am. Mineral.*, 1985, **70**, 1186–1192.
23 I. Norrbo, P. Gluchowski, I. Hyppänen, T. Laihinen, P. Laukkanen, J. Mäkelä, F. Mamedov, H. S. Santos, J. Sinkkonen, M. Tuomisto, A. Viinikanoja and M. Lastusaari, *ACS Appl. Mater. Interfaces*, 2016, **8**, 11592–11602.

24 R. D. Kirk, *Am. Mineral.*, 1955, **40**, 22–31.
25 I. Norrbo, P. Gluchowski, P. Paturi, J. Sinkkonen and M. Lastusaari, *Inorg. Chem.*, 2015, **54**, 7717–7724.
26 I. F. Chang, *J. Electrochem. Soc.*, 1974, **121**, 815–820.
27 S. Vuori, P. Colinet, I. Norrbo, R. Steininger, T. Saarinen, H. Palonen, P. Paturi, L. C. V. Rodrigues, J. Göttlicher, T. L. Bahers and M. Lastusaari, *Adv. Opt. Mater.*, 2021, **9**, 2100762.
28 I. Norrbo, A. Curutchet, A. Kuusisto, J. Mäkelä, P. Laukkanen, P. Paturi, T. Laihinen, J. Sinkkonen, E. Wetterskog, F. Mamedov, T. Le Bahers and M. Lastusaari, *Mater. Horiz.*, 2018, **5**, 569–576.
29 C. K. B. D. Vasconcelos and R. F. Bianchi, *Sens. Actuators, B*, 2009, **143**, 30–34.
30 S. Vuori, H. Byron, I. Norrbo, M. Tuomisto and M. Lastusaari, *J. Ind. Eng. Chem.*, 2023, **120**, 361–373.
31 B. M. Brau, Nepheline Syenite, in *The Canadian Encyclopedia*, Historica Canada, 2015.
32 A. S. Brioche, Feldspar and Nepheline Syenite, in *U.S. Geological Survey Minerals Yearbook*, 2018, pp. 1–10.
33 J. R. Carvajal, *Institut Laue-Langevin*, 2023, preprint.
34 R. W. W. Hooft, *COLLECT Data Collection Software*, Bruker AXS, Delft, The Netherlands, 2008.
35 Z. Otwinowski and W. Minor, *Methods Enzymol.*, 1997, **276**, 307–326.
36 O. V. Dolomanov, L. J. Bourhis, R. J. Gildea, J. A. K. Howard and H. Puschmann, *J. Appl. Crystallogr.*, 2009, **42**, 339–341.
37 G. M. Sheldrick, *Acta Crystallogr., Sect. C:Struct. Chem.*, 2015, **71**, 3–8.
38 G. M. Sheldrick, *Acta Crystallogr., Sect. A:Found. Crystallogr.*, 2008, **64**, 112–122.
39 J. Selverian, in *ColorCalculator*, OSRAM Sylvania, Beverly MA, 2022.
40 P. Colinet, H. Byron, S. Vuori, J. P. Lehtio, P. Laukkanen, L. V. Goethem, M. Lastusaari and T. L. Bahers, *Proc. Natl. Acad. Sci. U. S. A.*, 2022, **119**, 1–7.
41 K. T. Tait, E. Sokolova, F. C. Hawthorne and A. P. Khomyakov, *Can. Mineral.*, 2003, **41**, 61–70.
42 I. Hassan, S. M. Antao and J. B. Parise, *Am. Mineral.*, 2004, **89**, 359–364.
43 A. Lawrynowicz, S. Vuori, E. Palo, M. Winther, M. Lastusaari and K. Miettunen, *Chem. Eng. J.*, 2024, **494**, 153069.
44 E. Rehfuess, in *Global solar UV index: a practical guide*, World Health Organization, 2002.
45 A. A. Finch, H. Friis and M. Maghrabi, *Phys. Chem. Miner.*, 2016, **43**, 481–491.
46 C. Agamah, S. Vuori, P. Colinet, I. Norrbo, J. M. Carvalho, L. K. O. Nakamura, J. Lindblom, L. V. Goethem, A. Emmermann, T. Saarinen, T. Laihinen, E. Laakkonen, J. Lindén, J. Konu, H. Vrielinck, D. V. Heggen, P. F. Smet, T. L. Bahers and M. Lastusaari, *Chem. Mater.*, 2020, **32**, 8895–8905.
47 Deutsche Norm, *Phosphorescent Pigments and Products – Part 1: Measurement and Marking at the Producer*, 2009, pp. 1–16, DIN **67510-1**:2009-11.
48 W. A. Deer, R. A. Howie and J. Zussman, *Rock-Forming Minerals, Framework Silicates*, Geological Society of London, 2nd edn, 2004, vol. 4B.